RAPID COMMUNICATIONS

PHYSICAL REVIEW B VOLUME 43, NUMBER 16 1 JUNE 1991

Phase separation, charge-transfer instability, and superconductivity in the three-band extended Hubbard model: Weak-coupling theory

Yunkyu Bang and G. Kotliar
Serin Physics Laboratory, Rutgers University, Piscataway, New Jersey 08855-0849

C. Castellani, M. Grilli, and R. Raimondi
Dipartimento di Fisica, Universita di Roma "La Sapienza," I-00185 Roma, Italy
(Received 19 February 1991)

We study the interplay of charge-transfer instability and phase separation in the three-band model using the Hartree-Fock variational method for values of the interaction couplings comparable to the bandwidth. We establish that phase separation occurs near the region where previous weak-coupling calculations found s-wave superconductivity and a charge-transfer instability.

Several authors[1,2] have proposed the three-band extended Hubbard model as a minimal model describing the physical properties of the copper oxide layers in high-temperature superconductors. According to Varma, Schmitt-Rink, and Abrahams,[2] two ingredients are essential for attaining high-temperature superconductivity: (a) nearly equal values of the renormalized copper and oxygen orbital energies and (b) a nearest-neighbor copper and oxygen repulsion comparable with the hybridization energy. The effects of V as a pairing mechanism were analyzed by several authors. In the limit of zero hybridization, Hirsch *et al.*[3] and Trugman[4] argued that when V is much larger than the charge-transfer energy, the system undergoes phase separation. Littlewood and others[5-8] approached the problem in the weak-coupling limit. Using a random-phase-approximation expansion in all the interaction parameters, they found that increasing V causes the charge-transfer susceptibility to diverge. Close to this charge-transfer instability (CTI) they found extended s-wave and d-wave pairing. Grilli *et al.*[9] studied this problem in the limit of infinite on-site repulsion on copper for arbitrary values of charge-transfer energy and hybridization, using a large-N expansion which is not perturbative in any of the couplings. They argued that the CTI always drives the charge compressibility to infinity and found phase separation in the region of the phase diagram surrounding the metal-insulator transition.

Motivated by the results of Ref. 9, we reconsider in this paper the weak-coupling approach to the extended Hubbard Hamiltonian. Using a simple variational method, we look for phase separation in the three-band model. We also relate the phase separation to the charge transfer and the superconducting instability reported previously in the literature.

The Hamiltonian for the three-band model is the following:

$$\begin{aligned} H = & -t_{pd}^0 \sum_i [d_{i,\sigma}^\dagger (p_{xi,\sigma} - p_{-xi,\sigma} + p_{yi,\sigma} - p_{-y,\sigma}) + \text{H.c.}] \\ & + \varepsilon_d^0 \sum_{i,\sigma} d_{i,\sigma}^\dagger d_{i,\sigma} + \varepsilon_p^0 \sum_{i,\sigma} (p_{xi,\sigma}^\dagger p_{xi,\sigma} + p_{yi,\sigma}^\dagger p_{yi,\sigma}) \\ & + U \sum_{i,\sigma} n_{di,\uparrow} n_{di,\downarrow} + V \sum_{i,\sigma\sigma' a = \pm x, \pm y} n_{di,\sigma} n_{ai,\sigma'} \\ & + U_p \sum_{i,\sigma} (n_{xi,\uparrow} n_{xi,\downarrow} + n_{yi,\uparrow} n_{yi,\downarrow}) , \end{aligned} \tag{1}$$

where $d^\dagger$ and $p_{x,y}^\dagger$ are the creation operators of holes on Cu and O sites, respectively, $n_d = d^\dagger d$ and $n_a = p_a^\dagger p_a$, $\varepsilon_{d,p}^0$ is the Cu and O energy levels, t_{pd}^0 is the Cu-O hybridization, U is the on-site Cu repulsion, V is the nearest-neighbor Cu-O repulsion, and U_p is the on-site repulsion on O sites.

This work extends previous work by Coppersmith and Littlewood.[10] We follow these authors and use a Hartree-Fock variational wave function with two variational parameters, i.e., t (renormalized t_{pd}^0) and ε (renormalized $\varepsilon_p^0 - \varepsilon_d^0$). Although the renormalization of t_{pd}^0 is relatively small for parameters used in this paper,[11] the effect on the location of the phase-separation region and of the CTI is quite important. We express all energies in units of t_{pd}^0 throughout this paper.

The Hartree-Fock self-consistency equations are given by

$$\begin{aligned} \varepsilon = \varepsilon_p - \varepsilon_d &= \varepsilon_p^0 - \varepsilon_d^0 + 4V\langle n_d\rangle - 4V\langle n_p\rangle - U\langle n_d\rangle + \tfrac{1}{2} U_p \langle n_p\rangle \\ &= \varepsilon_p^0 - \varepsilon_d^0 - (\tfrac{1}{4} U - \tfrac{1}{8} U_p)(1+\delta) \\ &\quad + 4(V - \tfrac{1}{8} U - \tfrac{1}{16} U_p)(\langle n_d\rangle - \langle n_p\rangle) , \end{aligned} \tag{2}$$

$$t = t_{pd}^0 + V \sum_{k<k_f} \frac{t\gamma_k^2}{(\varepsilon^2 + 16 t^2 \gamma_k^2)^{1/2}} , \tag{3}$$

where

$$\langle n_d\rangle = \sum_{k<k_f} \frac{1}{2} + \frac{\varepsilon}{2(\varepsilon^2 + 16\gamma_k^2 t^2)^{1/2}} , \tag{4}$$

$$\langle n_p\rangle = \sum_{k<k_f} \frac{1}{2} - \frac{\varepsilon}{2(\varepsilon^2 + 16\gamma_k^2 t^2)^{1/2}} . \tag{5}$$

Here, $\langle n_d\rangle$ and $\langle n_p\rangle$ are the expectation values of n_d and $n_x + n_y$ per spin and per unit cell in our variational wave function and $\gamma_k = [\sin^2(k_x/2) + \sin^2(k_y/2)]^{1/2}$. To gain qualitative insight into the problem we used a spherical-band approximation which replaces γ_k by $[(k_x/\pi)^2 + (k_y/\pi)^2]^{1/2}$. We then checked that the results of the calculation do not change qualitatively when we solve (2) and (3) using the full band-structure value of γ_k. In the spherical-band approximation, Eqs. (2) and (3) reduce to[12]

$$\varepsilon=(\varepsilon_p^0-\varepsilon_d^0)-(U/4-U_p/8)(1+\delta)+\frac{\varepsilon}{t}(V-U/8-U_p/16)[\sqrt{2+\varepsilon^2/16t^2}-\sqrt{(1-\delta)+\varepsilon^2/16t^2}]\,, \tag{6}$$

$$t=t_{pd}^0+V/4(\{(2+\varepsilon^2/16t^2)^{3/2}-[(1-\delta)+\varepsilon^2/16t^2]^{3/2}\}/3-\varepsilon^2/16t^2[\sqrt{2+\varepsilon^2/16t^2}-\sqrt{(1-\delta)+\varepsilon^2/16t^2}])\,. \tag{7}$$

Here, $(1+\delta)/2=\langle n_d\rangle+\langle n_p\rangle$. Equations (6) and (7) can be used to study the instabilities of the model at fixed density and at fixed chemical potential. We consider the fixed density case first. Equation (6) resembles the mean-field equation for the magnetization in the Ising model. $(\varepsilon_p^0-\varepsilon_d^0)-(U/4-U_p/8)(1+\delta)$ plays the role of the external magnetic field and (n_d-n_p) is analogous to the magnetization order parameter. ε is analogous to the internal Weiss field. Its physical meaning is the renormalized energy difference between the copper and the oxygen orbitals and controls the valence of the system. The slope of the nonlinear function in the right-hand side of Eq. (6) at $\varepsilon=0$ plays the role of the magnetic-exchange interaction J divided by the temperature T. In our problem, J is given by $(V-U/8-U_p/16)$ and the temperature scale is set by t. The valence susceptibility $\chi_v=\partial(n_p-n_d)/\partial(\varepsilon_p^0-\varepsilon_d^0)$ at fixed doping δ corresponds to the Ising spin susceptibility. It diverges when the magnetic field is zero and the temperature is set equal to the critical value.[13] In our problem this occurs when

$$\frac{(V-U/8-U_p/16)(\sqrt{2}-\sqrt{1-\delta})}{t}=1 \tag{8}$$

and

$$(\varepsilon_p^0-\varepsilon_d^0)-(U/4-U_p/8)(1+\delta)=0\,. \tag{9}$$

Notice that increasing doping or increasing V is like increasing J/T in the Ising model and derives the system towards the valence instability (VI).

For fixed values of V, U, and U_p, Eq. (9) defines the VI line in Fig. 1 when the left-hand side of Eq. (8) is larger than 1. Across this line the valence ε jumps discontinuously. The VI line ends in a second-order transition point denoted by "×" in Fig. 1. As one approaches this point, the valence susceptibility diverges. Beyond the critical doping which is determined by Eq. (8), not all values of ε can be obtained by varying $\varepsilon_p^0-\varepsilon_d^0$. This point is illustrated in Fig. 2.

The Ising-model analogy describes the possible behaviors of ε for a given value of doping. It shows that close to the VI line there are two different solutions (where copper and oxygen have different valences) and that these solutions cross as one varies the doping across the VI line. Near this crossing the energy as a function of the total density has negative curvature and one has to investigate the concomitant phase separation. That is, we have to allow for fluctuations in the total density and calculate the response functions at a fixed chemical potential.

A typical plot of ε and t as a function of δ, showing discontinuous behavior, is shown in Fig. 3(a). For $\varepsilon_p^0-\varepsilon_d^0$ positive, ε increases with doping and jumps to a negative value at the VI line. The uniform compressibility $\chi=dn_{\rm tot}/d\mu$ is discontinuous and becomes negative for some range of hole concentration beyond the VI line [see Fig. 3(b)]. To understand this effect, one should note that ε obtained from the solution of the Hartree-Fock equations decreases rapidly in this regime. The O p level is mostly occupied and the Cu d level is almost empty. In this regime the renormalized kinetic energy is small and its increase with doping cannot compensate for the decrease of the Hartree shift Vn_d. Eventually U_p causes the chemical potential to increase as a function of doping. This effect is not very pronounced in Fig. 3(b) because we took a small value of U_p.

A detailed analysis of the mean-field equations shows that the VI point is surrounded by a region where compressibility is negative. This fine structure cannot be resolved in the phase diagram because this happens in a region very close to the VI point.

The VI point is therefore surrounded by a line (dashed line in Fig. 1) where $\partial\mu/\partial n_{\rm tot}$ is zero, and therefore the compressibility diverges. This is the CTI line, the line where the charge-transfer susceptibility $\partial(n_d-n_p)/\partial(\varepsilon_p^0-\varepsilon_d^0)$ at a fixed chemical potential and the compressibility simultaneously diverge.[14] This line also can be deter-

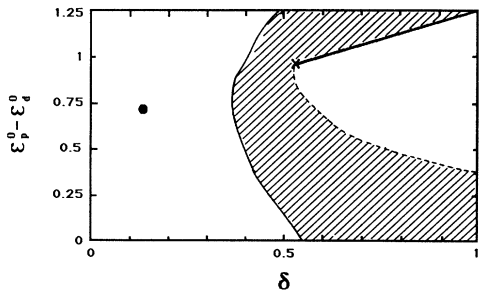

FIG. 1. Phase diagram for $U=3$, $V=2.5$, and $U_p=1$. The solid line is a line of the first-order transition ending in a VI critical point, "×". ε changes discontinuously across this line. The dashed line is a locus of the points where the compressibility diverges. The hatched area is obtained by Maxwell construction. The solid circle is the VI point without bandwidth renormalization.

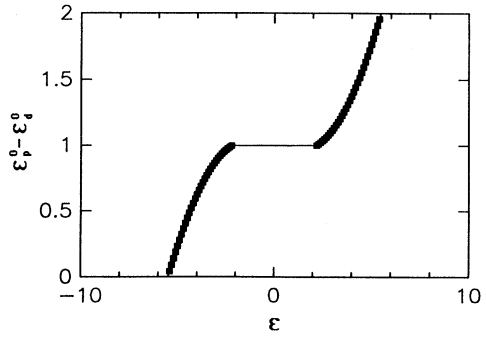

FIG. 2. Plot of $\varepsilon_p^0-\varepsilon_d^0$ vs ε (renormalized $\varepsilon_p^0-\varepsilon_d^0$) for $U=3$, $V=2.5$, $U_p=1$, and hole density=0.8 (0.5 is half filling). The physically allowed region is indicated by solid squares.

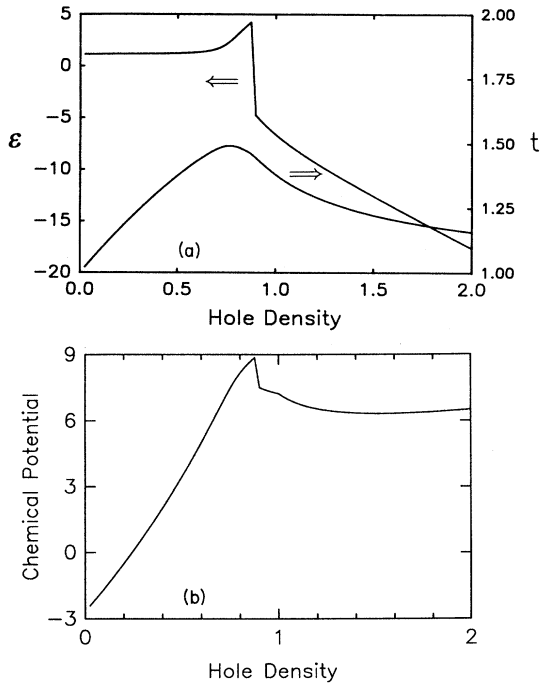

FIG. 3. (a) Plots of ε and t vs hole density for $U=3$, $V=2.5$, $U_p=1$, and $\varepsilon_p^0-\varepsilon_d^0=1.1$. (b) Plot of chemical potential vs hole density for the same parameters as in (a).

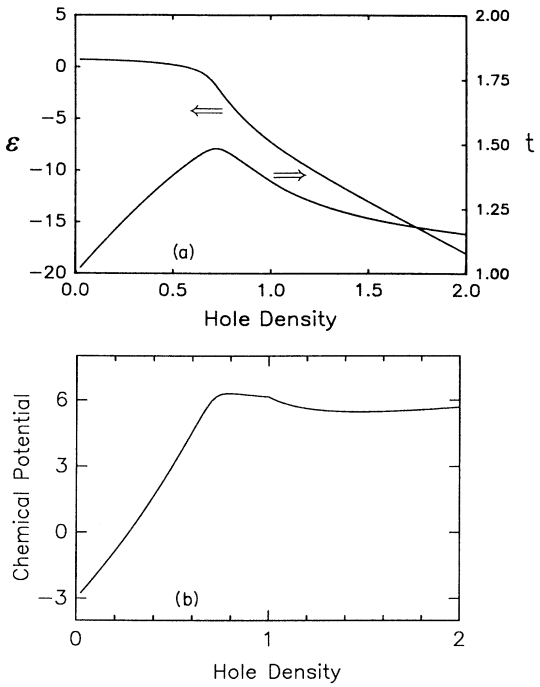

FIG. 4. (a) Plot of ε and t vs hole density for $U=3$, $V=2.5$, $U_p=1$, and $\varepsilon_p^0-\varepsilon_d^0=0.7$. (b) Plot of chemical potential vs hole density for the same parameters as in (a).

mined by looking for the divergence of the charge-transfer (CT) susceptibility calculated in the random-phase approximation along the lines of Ref. 5. Figures 4(a) and 4(b) show ε, t, and μ as a function of doping when $\varepsilon_p^0-\varepsilon_d^0$ is less than its critical value at the VI point. In this region of parameters, one crosses the CTI line (but not the VI line) as the doping increases, and the curves in Fig. 4 are continuous. The uniform compressibility and CT susceptibility diverge simultaneously when the CTI line is crossed, and beyond this line the uniform compressibility becomes negative for some range of hole density.

The divergence of the susceptibilities is preempted by phase separation. A Maxwell construction determines the region of the phase diagram which is not thermodynamically allowed. This is the hatched area in Fig. 1. The CTI line is therefore always surrounded by a phase-separation region after Maxwell construction.[9]

Many authors have investigated the role of V as a source of pairing in weak-coupling theory. The large N analysis of Ref. 9 has shown that superconductivity exists very near (but outside of) the phase-separation region. The close proximity of superconductivity and phase separation occurs in weak coupling as well. For example, in Ref. 8 Bang *et al.* found a region of the phase diagram where the interactions are attractive in the s-wave channel. Using the same values of the parameters U, V, U_p, and a renormalized charge-transfer energy $\varepsilon=0$ as in Ref. 8 the critical doping for VI in our calculation is $\delta_c=0.41$ (see Fig. 5). Since the calculations in Ref. 8 ignored the exchange diagrams, we also calculated the phase diagram of our model in the Hartree approximations (i.e., ignoring the renormalization of the hybridization).[15] Our Maxwell construction locates the phase separation (ps) along the line $\varepsilon=0$ at $\delta_{ps}=0.24$. Comparing the region of s-wave superconductivity (Fig. 2 in Ref. 8) with our Hartree phase diagram (Fig. 5) we find that part of the region where pairing occurs lies inside the phase-separation region.[16] A direct comparison of our phase diagram with the static calculations of Littlewood, Varma, and Abrahams[7] is not possible because these authors have included self-energy corrections in the determination of the phase diagram, effectively going beyond the Hartree-Fock approximation. It is interesting to notice that self-energy corrections actually increase the tendency towards charge-transfer instability.

One basic lesson to extract from our calculation is that

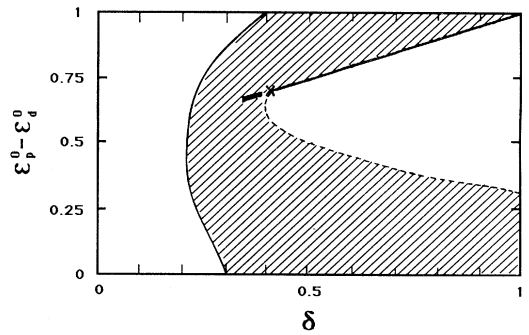

FIG. 5. Phase diagram with the same parameters as in Ref. 8, i.e., for $U=2$, $V=1.8$, and $U_p=0$. The notations are the same as in Fig. 1. The region where Ref. 8 calculates T_c is indicated by a thick solid line near the critical point.

the in-plane CT excitonic mechanism of superconductivity cannot operate too close to CTI, since that region is not thermodynamically allowed.[17]

In conclusion, we analyzed the VI, the CTI, and the phase separation in the three-band model using the Hartree-Fock approximation and obtained the phase diagram. Our result gives a clear picture of their interplay in the weak-coupling limit. It is therefore useful to emphasize how the qualitative features brought about by the nearest-neighbor repulsion V depend on having a small or a large U on the copper site (weak- or strong-coupling situations). In both limits, phase separation, superconductivity, and charge-transfer instability are all present when the hybridization energy and V are the same order of magnitude. The mathematical structure of the mean-field equations near the CTI boundary is very similar in both cases: the main effect of a large V is to allow for the coexistence of multiple valences. However, the instability in weak coupling is approached as one increases doping, while in strong coupling it can occur for arbitrary small doping. This is due to the existence of a metal-insulator transition at half filling in the large-U model. This is a nonperturbative effect in U and has no clear analog in the small-U limit. Because of the proximity to the Mott transition, the renormalized kinetic energy increases as the doping increases. Equation (6) shows that the opposite effect occurs in the weak-coupling limit. Except for this difference, one can now say that a coherent picture of the physics brought about by the nearest-neighbor repulsion emerges from the small- and large-U limit.

Note added. The phase diagram of $La_{2-x}Sr_xCuO_4$ obtained experimentally by Jorgensen *et al.*[18] agrees qualitatively with the prediction of our work.

We would like to thank E. Abrahams for many useful suggestions, a continued interest in this work, and for a careful reading of the manuscript. We also has useful discussions with K. Quader, C. Di Castro, P. B. Littlewood, and C. M. Varma. This work was supported by the National Science Foundation under Contract No. DMR 88-18713 and by the European Economic Community under Contract No. SC1*0222-C(EDB).

[1] V. J. Emery, Phys. Rev. Lett. **58**, 2794 (1987).

[2] C. M. Varma, S. Schmitt-Rink, and E. Abrahams, Solid State Commun. **62**, 681 (1987); in *Novel Mechanisms of Superconductivity,* edited by V. Kresin and S. Wolf (Plenum, New York, 1987), p. 355.

[3] J. E. Hirsch, E. Loh, Jr., D. J. Scalapino, and S. Tang, Phys. Rev. B **39**, 243 (1989).

[4] S. A. Trugman, Phys. Scr. **T27**, 113 (1989).

[5] P. B. Littlewood, C. M. Varma, S. Schmitt-Rink, and E. Abrahams, Phys. Rev. B **39**, 12 371 (1989).

[6] R. Putz, G. Dopf, B. Ehlers, L. Lilly, A. Muramatsu, and W. Hanke, Phys. Rev. B **41**, 853 (1990).

[7] P. B. Littlewood, C. M. Varma, and E. Abrahams, Phys. Rev. Lett. **63**, 2602 (1989).

[8] Y. Bang, K. Quader, E. Abrahams, and P. B. Littlewood, Phys. Rev. B **42**, 4865 (1990).

[9] M. Grilli, R. Raimondi, C. Castellani, C. Di Castro, and G. Kotliar, Int. J. Mod. Phys. B **5**, 309 (1991).

[10] S. N. Coppersmith and P. B. Littlewood, Phys. Rev. B **41**, 2641 (1990).

[11] $\langle d^\dagger p_x \rangle$ has maximum value ~ 0.2 for most of the parameters used in the text when $\varepsilon \sim 0$.

[12] In this approximation we replace the Brillouin zone by a circle of radius $\sqrt{2}\pi$ and rescale the density of points so as to have one state per unit cell.

[13] χ_v should not be confused with the charge-transfer instability χ_{ct} defined later in the text as the static susceptibility at fixed chemical potential describing the fluctuations of $n_d - n_p$ in the grand canonical ensemble.

[14] This can be easily seen by calculating the derivative of $n_d - n_p$ with respect to $\varepsilon_d^0 - \varepsilon_p^0$ at fixed chemical potential using the Maxwell relations.

[15] The Fock term reduces the phase separation and shifts the VI point.

[16] Calculation of T_c in Ref. 8 was done for $0.335 < \delta < 0.385$.

[17] It is, however, possible that allowing for pairing or improvement of the trial wave function in some other way may reduce or even eliminate the phase-separation region. See, for example, E. Cancrini, S. Caprara, C. Castellani, C. Di Castro, M. Grilli, and R. Raimondi, Europhys. Lett. (to be published).

[18] J. D. Jorgensen, P. Lightfoot, Shiyou Pei, B. Dabrowski, D. R. Richards, and D. G. Hinks (unpublished).